IL NUOVO CIMENTO **38 C** (2015) 63
DOI 10.1393/ncc/i2015-15063-8

Communications: SIF Congress 2014

Time-dependent measurement of the γ angle in the $B^0_s \to D^\pm_s K^\mp$ decay at LHCb

G. Tellarini

INFN, Sezione di Ferrara - Ferrara, Italy
Dipartimento di Fisica e Scienze della Terra, Università di Ferrara - Ferrara, Italy

received 15 May 2015

Summary. — This document describes the measurement of the weak phase γ in the $B^0_s \to D^\pm_s K^\mp$ decay performed by the LHCb experiment. The γ angle is the worst measured among the CKM unitarity triangle angles. The $B^0_s \to D^\pm_s K^\mp$ mode allows to measure γ in a very clean way since it decays through tree-level diagram avoiding the problem of the penguin pollution. The analysis is performed on the 2011 data sample collected by LHCb at the center of mass energy of 7 TeV, which corresponds to an integrated luminosity of $1\,\text{fb}^{-1}$. The relevant observables to be measured through the decay time dependence are the CP-violating coefficients C_f, S_f, $S_{\bar{f}}$, $A^{\Delta\Gamma}_f$, $A^{\Delta\Gamma}_{\bar{f}}$ since they depend on the γ angle. We find the CP observables to be: $C_f = 0.53 \pm 0.25 \pm 0.04$, $S_f = -1.09 \pm 0.33 \pm 0.08$, $S_{\bar{f}} = -0.36 \pm 0.34 \pm 0.08$, $A^{\Delta\Gamma}_f = 0.37 \pm 0.42 \pm 0.20$, $A^{\Delta\Gamma}_{\bar{f}} = 0.20 \pm 0.41 \pm 0.20$, where the uncertainties are statistical and systematic, respectively. We use these observables to perform the first measurement of γ in the $B^0_s \to D^\pm_s K^\mp$ decay mode, finding $\gamma = (115^{+28}_{-43})^\circ$ modulo 180° at 68% CL where both the statistical and systematic uncertainties are included.

PACS `29.20.db` – Storage rings and colliders.
PACS `29.90.+r` – Other topics in elementary-particle and nuclear physics experimental methods and instrumentation (restricted to new topics in section 29).

1. – Introduction

The $B^0_s \to D^\pm_s K^\mp$ decay can be described by two Feynman diagrams reported in fig. 1. One is a direct tree-level decay $\bar{B} \to f$ and the second is a tree-level decay where the original B meson oscillates to its anti-meson before decaying $\bar{B} \Rightarrow B \to f$. The sensitivity to the angle $\gamma \equiv \arg(-V_{ud}V^*_{ub}/V_{cd}V^*_{cb})$ of the unitarity triangle of the Cabibbo-Kobayashi-Maskawa (CKM) matrix is originated by the interference of the decay and $B^0_s - \bar{B}^0_s$ mixing amplitudes. The decay and mixing amplitudes of $B^0_s \to D^\pm_s K^\mp$ mode have the same order of magnitude in terms of the sine of the Cabibbo angle λ, allowing a large interference effect. Through a time-dependent analysis the CP-violating

© The Author(s)
Creative Commons Attribution 4.0 License (http://creativecommons.org/licenses/by/4.0)

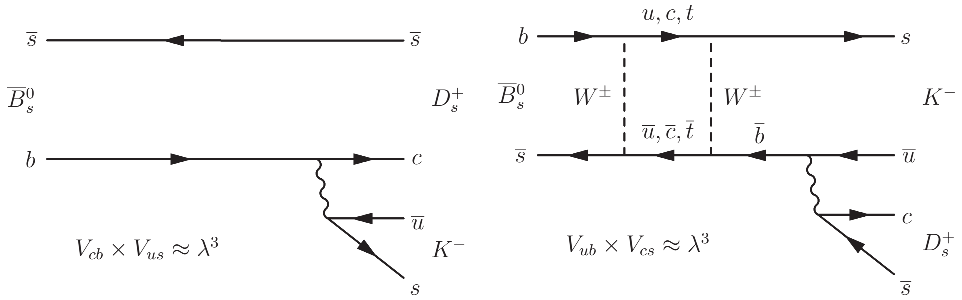

Fig. 1. – Feynman diagrams for $\bar{B}_s^0 \to D_s^+ K^-$ without (left) and with (right) mixing.

observables can be measured. They are functions of $\gamma - 2\beta_s$, where β_s is the B_s mixing phase, allowing to interpret the measurement in terms of γ or β_s by using an independent measurement of the other parameter as input. The time-dependent CP-asymmetry is defined as the difference between the B_s^0 and $\bar{B}_s^0$ decay rates to the same final state f(¹):

$$A_{CP}(t) = \frac{\Gamma_{B\to f}(t) - \Gamma_{\bar{B}\to f}(t)}{\Gamma_{B\to f}(t) + \Gamma_{\bar{B}\to f}(t)} = \frac{C_f \cos(\Delta m_s t) - S_f \sin(\Delta m_s t)}{\cosh(\frac{\Delta\Gamma_s}{2}t) - A_f^{\Delta\Gamma} \sinh(\frac{\Delta\Gamma_s}{2}t)}. \tag{1}$$

A similar equation can be written for the CP conjugate final state $\bar{f}$ replacing C_f by $C_{\bar{f}}$, S_f by $S_{\bar{f}}$ and $A_f^{\Delta\Gamma}$ by $A_{\bar{f}}^{\Delta\Gamma}$. The CP violating observables are defined as

$$\begin{aligned}
C_f &= \frac{1 - r_{D_sK}^2}{1 + r_{D_sK}^2} = -C_{\bar{f}}, \\
S_f &= \frac{2r_{D_sK} \sin(\delta - (\gamma - 2\beta_s))}{1 + r_{D_sK}^2}, \quad S_{\bar{f}} = \frac{-2r_{D_sK} \sin(\delta + (\gamma - 2\beta_s))}{1 + r_{D_sK}^2}, \\
A_f^{\Delta\Gamma} &= \frac{-2r_{D_sK} \cos(\delta - (\gamma - 2\beta_s))}{1 + r_{D_sK}^2}, \quad A_{\bar{f}}^{\Delta\Gamma} = \frac{-2r_{D_sK} \cos(\delta + (\gamma - 2\beta_s))}{1 + r_{D_sK}^2},
\end{aligned} \tag{2}$$

where $r_{D_sK} \equiv \mid A(\bar{B}_s^0 \to D_s^- K^+)/A(B_s^0 \to D_s^- K^+) \mid$, δ is the strong phase difference between the contributing diagrams and $\gamma - 2\beta_s$ is the weak phase difference.

The equality $C_f = -C_{\bar{f}}$ comes from the assumption of no CP violation neither in the decay nor in the mixing amplitudes, but only in the interference. This document reports the first measurement of the CP violating observables in $B_s^0 \to D_s^\pm K^\mp$ decays with the related evaluation of γ using a dataset corresponding to 1 fb^{-1} of integrated luminosity collected at $\sqrt{s} = 7$ TeV of pp collisions by the LHCb experiment. More information can be found in the corresponding paper [1].

(¹) In the following notation f corresponds to $D_s^- K^+$ and $\bar{f}$ to $D_s^+ K^-$

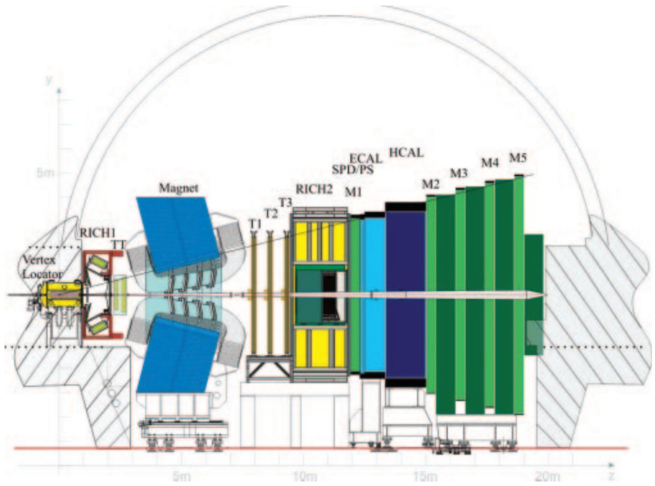

Fig. 2. – LHCb detector scheme.

2. – The LHCb detector

The LHCb detector shown in fig. 2 is one of the four main detectors of the Large Hadron Collider at CERN. It has been designed to study *CP* violation in beauty and charm hadrons decays produced by the proton-proton collisions. It is a single-arm forward spectrometer with a pseudorapidity covered between 2 and 5. It is characterized by an excellent vertex resolution provided by the VErtex LOcator (VELO). The detector includes a precise tracking system composed by the VELO itself and two other tracking stations before and after the dipole magnet providing momentum measurements. Different species of charged hadrons are identified by two Ring-Imaging CHerenkov detectors (RICH1 and RICH2) while a system of electromagnetic and hadronic calorimeters can identify high-energy photons, electrons and neutral pions. The identification of muons is provided by muon detectors placed downstream all the other sub-detectors and made alternating layers of iron and active material. A crucial role is played by the trigger system which is composed by a hardware stage and by a software system. The hardware trigger is based on the information from the calorimeter and muon systems then the software trigger applies a full event reconstruction.

3. – Data sample, selection and analysis

Starting from the reconstructed charged particles, the following D_s decays are selected: $D_s^- \to K^- K^+ \pi^-$, $D_s^- \to K^- \pi^+ \pi^-$, $D_s^- \to \pi^- \pi^+ \pi^-$. These D_s^- candidates are subsequently combined with a companion particle to form the $B_s^0 \to D_s^- K^+$ or the $B_s^0 \to D_s^- \pi^+$ decay modes. The decay time and B_s^0 mass resolutions are improved by performing a kinematic fit in which the B_s^0 candidate is constrained to originate from its associated proton-proton interaction point. In addition the B_s^0 mass is evaluated constraining the D_s mass to the current PDG value. The combinatorial background is suppressed by a gradient boosted decision tree which is an implementation of the TMVA software package. A crucial role to reduce backgrounds is played by the particle identification (PID). Different PID requirements are used in order to reduce peaking backgrounds from other b-hadrons and c-hadrons decays.

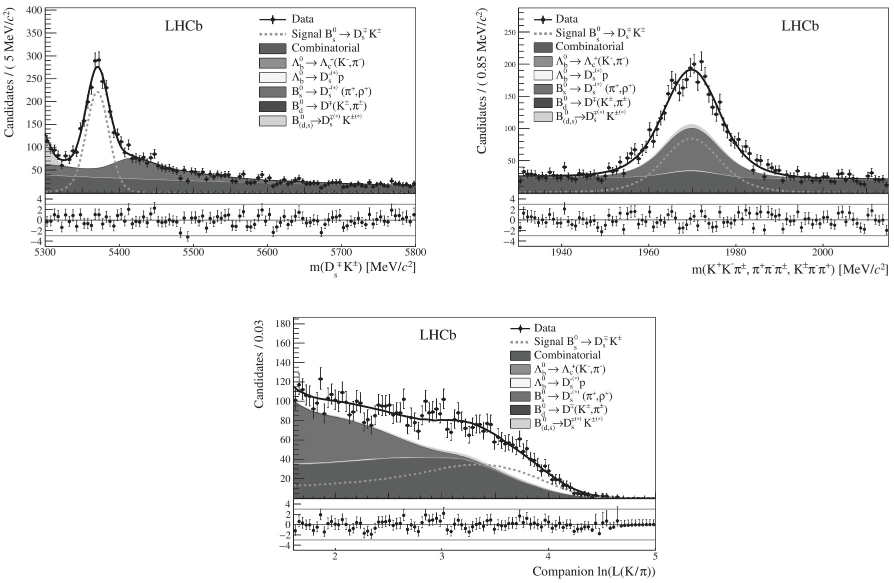

Fig. 3. – Simultaneous fit from left to right to B_s^0 invariant mass distribution, D_s invariant mass distribution and ID of the companion kaon.

To measure the CP-violating observables it is necessary to perform a fit to the decay time distribution of the selected $B_s^0 \to D_s^{\pm}K^{\mp}$ candidates. The $B_s^0 \to D_s^-\pi^+$ decay is used as a control mode for the optimization of the selection (differing only for the requirement on the ID of the companion particle from kaon to pion), for studying and constraining the physics backgrounds and for the flavour tagging algorithms calibration.

3·1. *Analysis strategy.* – In order to get a better discrimination between signal and background events a simultaneous fit is performed on the B_s and D_s invariant masses and also on the ID of the companion kaon. In addition to the combinatorial background, partially reconstructed and mis-identified events are present in the selected sample. The plots of the multidimensional fit are shown in fig. 3; 1770 ± 50 signal events are found for the $B_s^0 \to D_s^{\pm}K^{\mp}$ decays. Two different approaches have been developed for the time-dependent fit. One is based on the sPlot technique (*sFit*) [2] to subtract the background and uses the signal weights from the multidimensional fit. Following this *sFit* approach the time-dependent fit is essentially a fit to a pure signal sample. The other approach is a classical fit (*cFit*) where each background has to be properly modeled also in its decay time evolution. A necessary ingredient of the time fit to $\Gamma_{B\to f}(t)$ and $\Gamma_{\bar{B}\to f}(t)$ is the knowledge of the initial B flavour (B_s^0 or $\bar{B_s^0}$). In both fitting approaches, *sFit* and *cFit*, the flavour information of the neutral B_s meson at production time is provided by the combination of two independent taggers, Same Side Kaon and Opposite Side. The Same Side Kaon (SSK) tagger exploits the charge of the fragmentation kaon track accompanying the B_s^0 signal meson. The Opposite Side (OS) tagger uses an inclusive reconstruction of the non signal B hadron decay since in the $b\bar{b}$ production two beauty hadrons are always produced: one is identified as signal, the other one can be used to infer the production flavour. The overall tagging efficiency is $\epsilon_{tag} \approx 67.5\%$. The decision on the flavour of the B meson provided by the tagging algorithm can be wrong due to the wrong identification of the tagging particle or due to mixing of neutral B for the

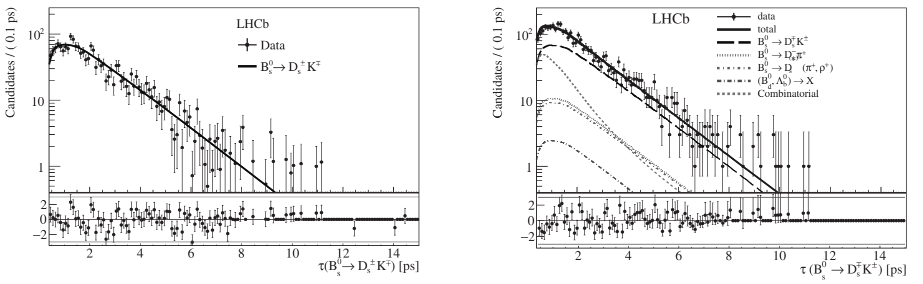

Fig. 4. – Result of the decay time (on the left side) *sFit* and (on the right side) *cFit* to the $B_s^0 \to D_s^\pm K^\mp$ candidates.

OS tagger. The tagging algorithms provide an estimate of the probability of mistag η based on a neural network which is used in the fit to weight the events. The estimated mistag has to be calibrated on data where a linear relation $\omega = p_0 + p_1 \cdot (\eta - <\eta>)$ between the predicted and the measured mistag probability is used. For this analysis the tagging calibration is done using the flavour-specific $B_s^0 \to D_s^- \pi^+$ decay for the SSK tagger while for the OS is used the calibration obtained by several control channels. The tagging parameters p_0, p_1 and $\langle \eta \rangle$ are used in the fit as input parameters with Gaussian constraints. The flavour tagging has a non-negligible impact on the CP observables measurement since the statistical uncertainty scales as $1/\sqrt{\epsilon_{tag} D^2}$, where $\epsilon_{tag} D^2$ is the tagging power and $D = 1–2\omega$ is the dilution due to the imperfect tagging. The tagging power of the SSK and OS combination is of about 5.07%.

The decay time resolution should be described as well as possible since any mismodelling of the resolution function could bias the measurement of the CP violation observables. In the analysis the decay time error is used as an estimate of the time resolution event by event. The overall resolution corresponds to 47 fs. The events selection introduces a time-dependent acceptance effect which has to be included in the fit. The decay time acceptance function is evaluated using the $B_s^0 \to D_s^- \pi^+$ data sample and corrected for differences with the $B_s^0 \to D_s^\pm K^\mp$ decay by acceptances ratio $B_s^0 \to D_s^\pm K^\mp / \ B_s^0 \to D_s^- \pi^+$ in simulation. The parameters of the acceptance function are fixed in the $B_s^0 \to D_s^\pm K^\mp$ fit. As a crosscheck of the whole analysis procedure, the mixing frequency Δm_s is measured in the $B_s^0 \to D_s^- \pi^+$ data sample, finding $\Delta m_s = 17.772 \pm 0.022\,\mathrm{ps}^{-1}$ which is in perfect agreement with the published LHCb result $\Delta m_s = 17.768 \pm 0.024\,\mathrm{ps}^{-1}$ [3].

The other inputs for signal and backgrounds events as Γ_s, $\Delta\Gamma_s$, $\Gamma_{\Lambda_b^0}$ and Γ_d are taken from independent measurements done by LHCb.

3˙2. *Results.* – Both fitters use an unbinned maximum likelihood fit to the CP observables defined before. Except for the CP observables, all the other parameters are constrained in the fit.

In fig. 4 the fit to the decay time distribution is shown: on the left plot the *sFit* is reported while on the right plot the *cFit* is reported. In table I the result of the decay time fit is reported for both the fitters. The statistical and systematic uncertainties are quoted for each CP observable. The main systematic uncertainties are due to the fixed parameters of the fit: Δm_s, Γ_s and $\Delta\Gamma_s$ and from the limited knowledge of the decay time resolution and acceptance. In order to estimate these uncertainties a large set of pseudoexperiments is used. The pseudoexperiments are generated with the average of the

TABLE I. – *Fitted values of the CP observables to the* $B_s^0 \to D_s^{\pm} K^{\mp}$ *decay time distribution. The statistical and systematic uncertainties are also quoted.*

Parameter	*sFit* fitted value	*cFit* fitted value
C_f	$0.52 \pm 0.25 \pm 0.04$	$0.53 \pm 0.25 \pm 0.04$
$A_f^{\Delta\Gamma}$	$0.29 \pm 0.42 \pm 0.17$	$0.37 \pm 0.42 \pm 0.20$
$A_{\bar{f}}^{\Delta\Gamma}$	$0.14 \pm 0.41 \pm 0.18$	$0.20 \pm 0.41 \pm 0.20$
S_f	$-0.90 \pm 0.31 \pm 0.06$	$-1.09 \pm 0.33 \pm 0.08$
$S_{\bar{f}}$	$-0.36 \pm 0.34 \pm 0.06$	$-0.36 \pm 0.34 \pm 0.08$

TABLE II. – *Systematic uncertainties related to the sFit results expressed as fractions of the statistical uncertainties.*

Source	C_f	S_f	$S_{\bar{f}}$	$A_f^{\Delta\Gamma}$	$A_{\bar{f}}^{\Delta\Gamma}$
Δm_s	0.062	0.104	0.100	0.013	0.013
Time resolution	0.104	0.092	0.096	0.004	0.004
Acceptance Γ_s, $\Delta\Gamma_s$	0.043	0.039	0.038	0.427	0.437
Sample splits	0.124	0.072	0.071	0.000	0.000
Total	0.179	0.161	0.160	0.427	0.437

TABLE III. – *Systematic uncertainties related to the cFit results expressed as fractions of the statistical uncertainties.*

Source	C_f	S_f	$S_{\bar{f}}$	$A_f^{\Delta\Gamma}$	$A_{\bar{f}}^{\Delta\Gamma}$
Δm_s	0.068	0.131	0.126	0.014	0.011
Time resolution	0.131	0.101	0.103	0.004	0.004
Acceptance Γ_s, $\Delta\Gamma_s$	0.050	0.050	0.043	0.461	0.464
Sample splits	0.102	0.156	0.151	0.000	0.000
Total	0.187	0.234	0.226	0.466	0.470

cFit and *sFit* central values and subsequently they are processed by the full data fitting procedure where each parameter is varied according to its systematic uncertainty. The difference with the nominal fit is considered as systematic uncertainty. The uncertainties related to the tagging parameters are already included in the statistical errors.

The decay time acceptance mostly affects the CP coefficients related to the hyperbolic terms of the decay rate. An increase in the statistics of the $B_s^0 \to D_s^- \pi^+$ would improve the description of the acceptance function. Further studies have been done splitting the data sample into two subsets according to the two magnet polarities and the hardware trigger decision. In tables II and III we report the systematic uncertainties in terms of the statistical uncertainties, respectively, for the *sFit* and for the *cFit* results. The *cFit* and *sFit* results are in good agreement and differences between the two fitters are evaluated from the distributions of the per-pseudoexperiment differences of the fitted values. Both fitters return compatible results.

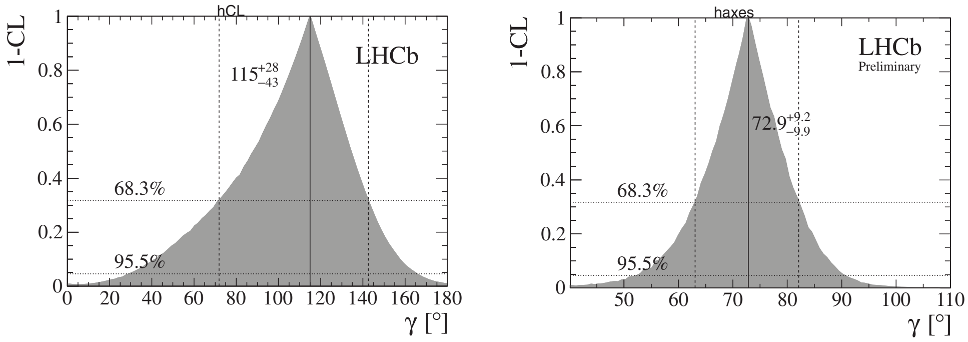

Fig. 5. – Graph showing the 1-CL for γ in the $B_s^0 \to D_s^{\pm}K^{\mp}$ decay mode (left) and using all the tree-level measurements performed by LHCb (right) [5].

3˙3. *The* γ *angle extraction.* – In order to extract the value of the γ angle, the *cFit* results have been arbitrarily chosen. The method consists in maximizing a likelihood including the physics parameters: γ, $\phi_s \to -2\beta_s$, r_{D_sK}, δ and the CP violating observables expressed through eq. (2). The value of γ as well as that of r_{D_sK} and δ are determined by this likelihood maximization while the value of ϕ_s is fixed to an independent measurement performed by LHCb [4]. We obtain $\gamma = (115^{+26}_{-35}(\text{stat})^{+8}_{-25}(\text{syst}) \pm 4\ (\phi_s))^{\circ}$ at 68% Confidence Level (CL), where the intervals are expressed modulo 180°. The graphs in fig. 5 show 1-CL for γ. The left-side plot refers to the measurement of γ performed in the $B_s^0 \to D_s^{\pm}K^{\mp}$ decay mode. The LHCb experiment has measured the γ angle also in other tree-level processes such as $B^+ \to DK^+, D\pi^+$ and $B^0 \to D^0K^{*0}$ using different techniques: ADS, GLW, GLS, GGSZ. The combination of all the tree-level measurements provide a value for $\gamma = (72.9^{+9.0}_{-10.0})^{\circ}$ at 68% CL [5]. The right-side plot in fig. 5 is the 1-CL graph for γ as a result of the combination of all the tree-level measurements performed by LHCb. The contribution of the $B_s^0 \to D_s^{\pm}K^{\mp}$ measurement to the combination is small for the moment. It represents an additional independent way to measure γ and it will contribute mostly given the enhancement in statistics of the next analysis with $\int \mathcal{L} = 3\,\text{fb}^{-1}$.

REFERENCES

[1] LHCb Collaboration, *Measurement of CP asymmetry in* $B_s^0 \to D_s^{\pm}K^{\mp}$ *decays J. High Energy Phys.*, **11** (2014) 060.

[2] Yuehong Xie, *sFit: a method for background subtraction in maximum likelihood fit* arXiv:0905.0724 (2009).

[3] LHCb Collaboration, *Precision measurement of the* $B_s^0 - \bar{B}_s^0$ *oscillation frequency with the decay* $B_s^0 \to D_s^- \Pi^+$. *New J. Phys.*, **15** (2013) 053021.

[4] LHCb Collaboration, *Measurement of CP violation and the* B_s^0 *meson decay width difference with* $B_s^0 \to J/\Psi K^+K^-$ *and* $B_s^0 \to J/\Psi\pi^+\pi^-$ *decays.* arXiv:1304.2600 (2013).

[5] LHCb Collaboration, *Improved constraints on* γ*: CKM2014 update* 8th International Workshop on the CKM Unitarity Triangle, Univ. Tech., Vienna, Austria, 08 - 12 Sep 2014.